

Arsenic-induced etched nanovoids on GaSb (100)

S. H. Huang,^{a)} G. Balakrishnan, M. Mehta, L. R. Dawson, and D. L. Huffaker^{b)}
*Center for High Technology Materials, University of New Mexico, 1313 Goddard SE,
 Albuquerque, New Mexico 87106*

P. Li

Department of Earth and Planetary Science, University of New Mexico, Albuquerque, New Mexico 87131

(Received 5 March 2007; accepted 6 July 2007; published online 28 August 2007)

We describe *in situ* nanoscale etch-pit formation on GaSb (100) surfaces as a result of exposure to an As₂ flux in molecular beam epitaxy. The pits form as a result of an Sb-displacement reaction that occurs between the GaSb substrate and the impinging As adatoms. The nanoscale surface features are highly crystallographic with a strong preference for {111} planes, similar to other etching techniques. Nanopit dimensions and density increase with As exposure time. For the 60 s exposure analyzed in this article, the pits vary in both size and shape with average dimensions ~ 25 nm wide and 50–80 nm long and 10–70 nm deep, with density of $\sim 1 \times 10^9/\text{cm}^2$. Subsequent GaAs overgrowth proceeds by a coalescence mechanism leaving interfacial nanovoids and finally highly planar bulk layers. © 2007 American Institute of Physics. [DOI: 10.1063/1.2772532]

I. INTRODUCTION

While most etching processes used in semiconductor device fabrication are performed *ex situ* and involve the removal of several microns of materials,¹ more novel *in situ* etch processes are also under development for nanoscale applications. These include nanochannel formation,² delineation of nanopatterns for novel quantum structure formation^{3,4} and flash memory device fabrication.⁵ Etching and surface patterning on a nanoscale is presently achieved through *e*-beam lithography,^{6–9} scanning tunneling microscopy assisted lithography,^{10,11} optical lithography¹² and *in situ* processes such as Bromine-based molecular beam epitaxy (MBE) etches of III-As compounds.¹³ The *in situ* etch techniques have a distinct advantage over the *ex situ* techniques for regrowth processes since the surface is free of contaminants and native oxides. These *in situ* etch techniques have improved to the extent that even complex tasks such as dielectric mask removal can be achieved without removing samples from growth reactors.¹⁴

In this article, we demonstrate a method for etching GaSb nanopits *in situ* within a MBE system using As₂ as a reactant. Because As₂ is a common source in most III-V machines, this process facilitates GaSb *in situ* etching without complex equipment modifications. Subsequent GaAs overgrowth proceeds by coalescence over the etched pits which results in nanovoids at the GaAs/GaSb interface followed by planar bulk material growth. The highly faceted nanovoids may also offer encapsulation schemes for the formation of novel quantum-confined ensembles.³ The dimensions of the voids ensure quantum size effects for the encapsulated material.

The GaSb solubility in the As-rich ambient is attributed to a negative enthalpy of reaction as noted by Losurdo *et al.*¹⁵ The As₂ specie aggressively reacts with the GaSb for

both (1) the anion exchange reaction and (2) the isoelectronic AsSb compound formation reaction where (1) $2\text{GaSb} + \text{As}_2 \rightarrow 2\text{GaAs} + \text{Sb}_2$, $\Delta H^\circ = -47.6$ kJ/mol and (2) $\text{GaSb} + \text{As}_2 \rightarrow \text{GaAs} + \text{AsSb}$, $\Delta H^\circ = -33.9$ kJ/mol. In both reactions, the As₂ strongly reacts with the GaSb to produce a GaAs and either excess Sb (1) or AsSb (2). In the study described here, we establish that the As₂ reactions can be used to etch GaSb surfaces and that the etch process results in faceted pits, very similar to other etching processes.^{16–18} We analyze and characterize the As₂-based etch process at the GaSb surface using high resolution scanning electron microscopy (HRSEM). We then analyze bulk GaAs overgrowth as a function of coverage. Atomic force microscopy (AFM) and transmission electron microscopy (TEM) images establish the process of coalescence that initially caps the interfacial pits forming nanovoids and finally results in planar bulk GaAs.

II. EXPERIMENTAL DETAILS

The samples for interfacial analysis are grown in a V80H MBE reactor with valved crackers for both the As and the Sb source. The crackers are operated at 900 °C and 950 °C respectively resulting in As₂ and Sb₂ species. The temperature of the substrate is determined using a pyrometer while growth surface is monitored through a reflective high-energy electron beam (RHEED) system in conjunction with a KSA™ RHEED analysis. The growth is initiated on a GaSb substrate with a thermal oxide desorption process at ~ 540 °C followed by a GaSb smoothing layer at 510 °C. The GaSb is grown with a III:V beam equivalent pressure (BEP) ratio of 1:6. The RHEED pattern is used to verify a (3 × 1) pattern indicative of extremely smooth GaSb. At this point, the growth is paused and excess Sb is desorbed from the GaSb surface. Next, the surface is subjected to an As₂ overpressure with an approximate beam equivalent pressure of 1×10^{-6} mTorr with the substrate at 510 °C. The exposure of the As₂ results in the transformation of the RHEED from a (3 × 1) to an unidentifiable “murky” pattern. The rem-

^{a)}Electronic mail: huangsh@unm.edu

^{b)}Electronic mail: huffaker@cht.unm.edu

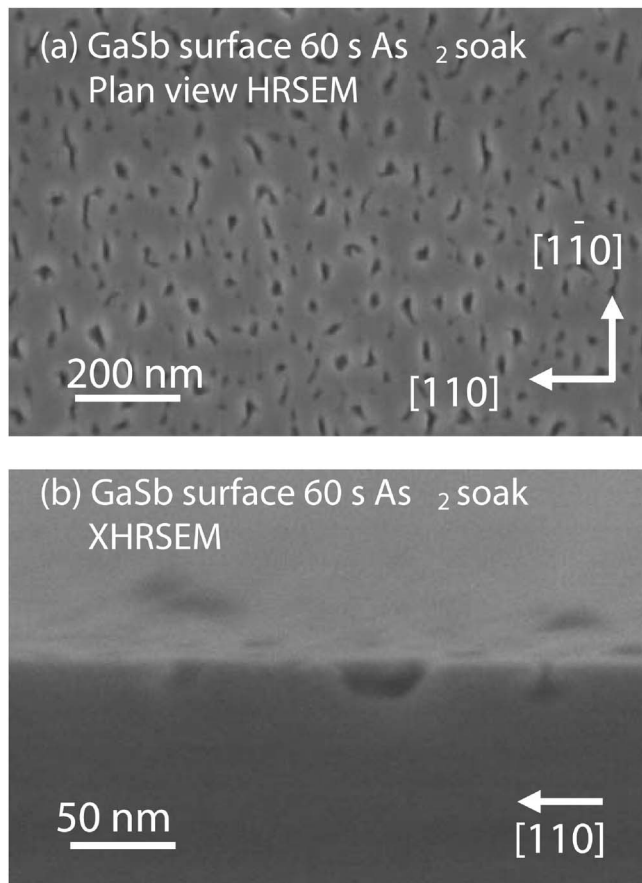


FIG. 1. HRSEM images featuring etch pits on the GaSb surface after 60 s As_2 soak (a) plan view, (b) side view.

nants of the (3×1) reconstructions disappear after a 60 s As_2 soak. The GaAs growth is then initiated without any changes in the growth temperature resulting in a smoothing of the surface with continued growth for ~ 20 nm. The III:V BEP ratio for the GaAs growth is 1:10.

A Hitachi S-5200 SEM system is used to analyze the As_2 induced etch pits on the GaSb surface through plan-view and side-view images. High-resolution or cross section TEM (XTEM) specimens are prepared by mechanically grinding samples to a thickness of less than $10 \mu\text{m}$ and then using an ion beam to thin the samples to electron transparency. A JEOL 2010 system is used for TEM analysis and images are produced in both bright-field (BF) and dark-field (DF) modes. The BF images elucidate void faceting and evolution of the GaAs overgrowth on the etched GaSb surface. The DF images analyze epitaxial quality.

III. RESULTS AND DISCUSSION

Figure 1 shows the SEM images of the GaSb surface after a 60 s As_2 soak [(a) plan view, (b) side view]. The pits vary in both size and shape with average dimensions of ~ 25 nm in width and 50–80 nm in length and 10–70 nm in depth, with a pit density of $\sim 1 \times 10^9/\text{cm}^2$. There appears to be no significant directionality to the pit orientation. The side view (b) shows the image of the (110) cleaved facet with a 30 nm wide pit intercepted by the cleaving plane. While the resolution available using the HR-SEM is not sufficient to

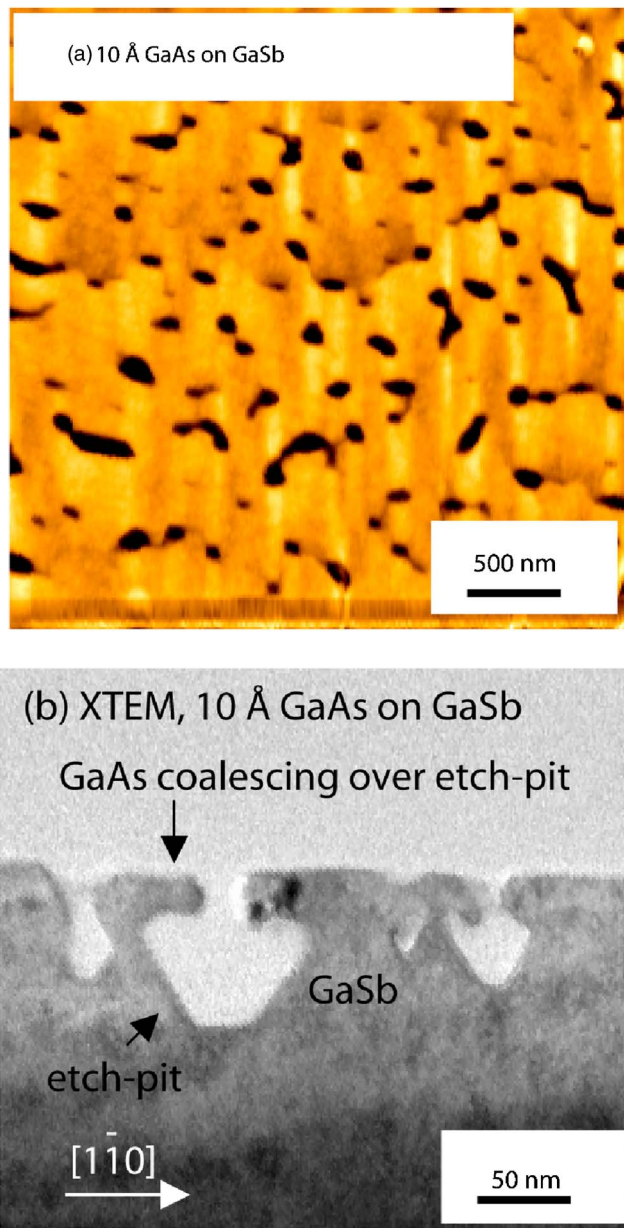


FIG. 2. GaAs (10 \AA) overgrowth on GaSb surface. (a) AFM image and (b) XTEM image showing partial GaAs coalescence over etched pits.

resolve the faceting of the pits, the images correlate the pit structure from the surface to the cross section as a result of As_2 reaction with the GaSb substrate.

Figures 2 and 3 show AFM and TEM images that elucidate the faceted voids and evolution of the GaAs overgrowth on the etched GaSb surface with increased GaAs coverage from 3 to 30 MLs. Figure 2(a) shows the AFM image after 10 \AA (~ 3 MLs) of GaAs deposition on a GaSb surface exposed to As_2 for 60 s. The AFM image shows surface remnants of the etched pits as dark features and suggests only partial GaAs coalescence over the pit after the 3 ML deposition. The image shows a pit density of $1 \times 10^9/\text{cm}^2$, which is consistent with that observed in Fig. 1(a). Figure 2(b) shows a cross section TEM image of the same sample and elucidates the lateral progression of the overgrowth process. With continued GaAs deposition, the lateral overgrowth pro-

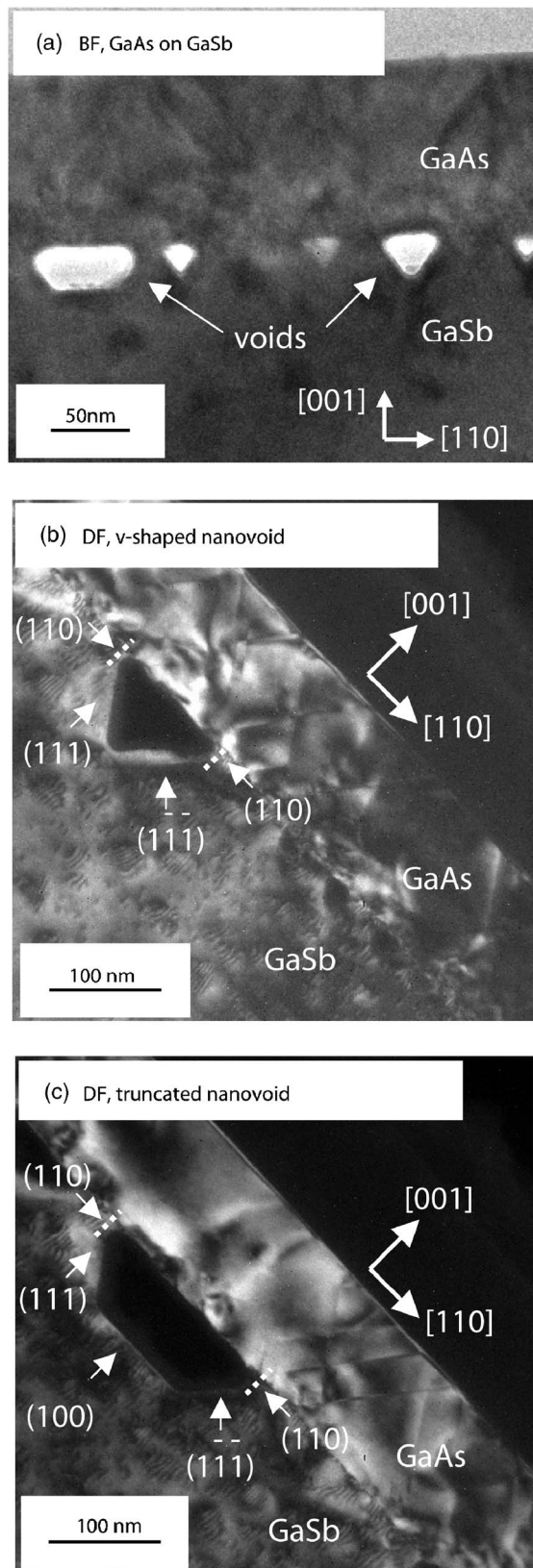


FIG. 3. XTEM images of GaAs/GaSb interface (a) bright field (BF) image featuring nanovoids, (b) (220) dark field (DF) image showing a single *v*-shaped nanovoid (c) (220) DF image showing a single truncated *v*-shaped nanovoid.

ceeds to coalesce over the pits forming encapsulated nanoscale voids at the interface. This image further indicates that no GaAs growth occurs inside the etch pits.

Figures 3(a)–3(c) shows a TEM analysis of a completely coalesced GaAs (100 nm) cap layer, grown on the GaSb pitted surface. Both BF and DF analyses are included. Figure 3(a) shows a BF image of the GaAs/GaSb interface featuring both *v*-shaped and truncated nanovoids. In the BF image, the voids appear white surrounded by the darker III-V matrix and the limiting crystal planes can be clearly measured. The *v*-shaped nanovoid is limited by (111) and (11 $\bar{1}$) planes on each side while the truncated *v*-shaped nanovoid, also enclosed by (111) and (11 $\bar{1}$) sidewalls, is bound by a (100) plane in the bottom. A closer inspection of the etched voids in the figure also shows a hint of the {110} planes near the surface. The formation of the facets are strongly determined by the etch rates along specific crystallographic directions resulting in low-index facets. Various experiments have shown that the etch rate for the low-index crystal planes is in the order of (111)*B* > (100) > (110). This directional etching progression has been well documented in III-V materials.^{17,18}

Figures 3(b) and 3(c) show (220) DF TEM images of the GaAs/GaSb interface and elucidate features in the coalesced GaAs overgrowth. As we pointed out above, the GaAs nucleates on the unetched GaSb surface and proceeds via lateral overgrowth to coalesce over the pits forming encapsulated nanovoids. The large mismatch between the GaAs epilayer and GaSb is relaxed through defects or threading dislocations. Figure 3(b) shows a significant threading dislocation density in the GaAs overgrowth that originates at both the GaAs/GaSb interface region and the laterally overgrown cap material over the void. The threading dislocations seem to cluster at certain points in the image where the GaAs coalesces.¹⁹ Figure 3(c) shows a similar DF image of the GaAs coalescence over a truncated void. The truncated void in Fig. 3(c) is larger in dimension than the one in Fig. 3(b) and the GaAs cap layer seems to possess a lower defect density. This effect could be attributed to the fact that the larger voids result in a larger area of GaAs not in contact with the mismatched GaSb, thus resulting in more effective strain-relief and subsequently lower defect density.

Figures 4(a) and 4(b) show high-resolution TEM images of two different nanovoids and their respective surrounding material. Figure 4(a) indicates the presence of amorphous material in the interior of the void, which appears as a thick coating on the {111} planes. The amorphous material does not produce any TEM diffraction pattern and could either be excess Sb as a result of the anion exchange reaction as described by (1) or the isoelectronic AsSb compound as a result of the alternate reaction (2). The amorphous elemental Sb or AsSb layer probably decreases and limits the etching rate in {111} planes.²⁰ Once the surface AsSb or Sb layer accumulates to some extent, the etch rate in the [110] could be faster than that in the [100] direction leading the pit to widen faster than it deepens and thus resulting in a (100) plane in the bottom and the formation of truncated *v*-shaped pits. The amorphous deposition also seems to prevent crystallographic adatom incorporation on the {111} planes. Thus, the lateral GaAs overgrowth may proceed from the (110) planes to coa-

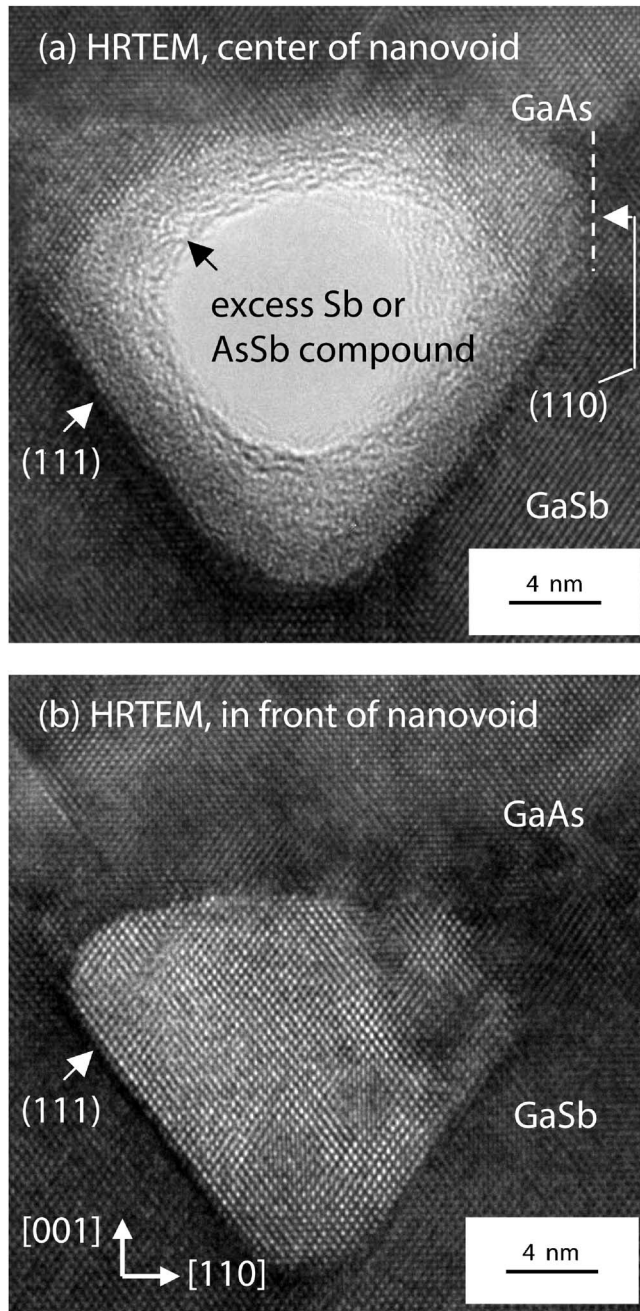


FIG. 4. HR-XTEM images of (a) a single nanovoid with amorphous surface coating, and (b) nanovoid viewed through several atomic layers showing crystalline structure.

lesce over the pit. While the overgrowth process is indicated in Fig. 2(b), the (110) nucleation site can only be seen in the higher-resolution image shown in Fig. 4(a).

An alternate high-resolution XTEM in Fig. 4(b) shows a nanovoid viewed through several atomic layers in front of the void. This image allows for only the crystalline material

in front of the nanovoid to be seen, since the amorphous material is hidden from view. We can now very clearly see that the terminating facets are the {111} planes and that the nucleation occurs on the (110) planes. The nanovoid region appears much lighter in contrast to the surrounding material due to the difference in material thickness.

IV. CONCLUSIONS

In conclusion, we demonstrate an *in situ* etch process of a GaSb surface in an As_2 overpressure which results in nanoscale pits on the exposed GaSb surface. The etch process is attributed to both the anion exchange reaction and the isoelectronic AsSb compound formation reaction between the As_2 and GaSb surface. Images of the etched GaSb surface indicate that the nanoscale pits are highly faceted and that the facets are terminated with a layer of amorphous material. Subsequent GaAs capping proceeds via lateral overgrowth and coalescence to form nanovoids at the interface. This *in situ* etch process applied to a masked surface may be technologically useful to define a patterned array of uniformly etched nanovoids.

- ¹S. A. Campbell, *The Science and Engineering of Microelectronic Fabrication* (Oxford University Press, Oxford, 1996).
- ²D.-Y. Xia and S. R. J. Brueck, *J. Vac. Sci. Technol. B* **23**, 2694 (2005).
- ³M. H. Baier, S. Watanabe, E. Pelucchi, and E. Kapon, *Appl. Phys. Lett.* **84**, 1943 (2004).
- ⁴S. Birudavolu, N. Nuntawong, G. Balakrishnan, Y. C. Xin, S. Huang, S. C. Lee, S. R. J. Brueck, C. P. Hains, and D. L. Huffaker, *Appl. Phys. Lett.* **85**, 2337 (2004).
- ⁵K. R. Lensing, C. Miller, G. Chudleigh, B. Swain, M. Laughery, and A. Viswanathan, *Proc. SPIE* **5375**, 307 (2004).
- ⁶W. Daschner, M. Larsson, and S. H. Lee, *Appl. Opt.* **34**, 2534 (1995).
- ⁷T. S. Yeoh, R. B. Swint, A. Gaur, V. C. Elarde, and J. J. Coleman, *IEEE J. Sel. Top. Quantum Electron.* **8**, 833 (2002).
- ⁸D. Chithrani, R. L. Williams, J. Lefebvre, P. J. Poole, and G. C. Aers, *Appl. Phys. Lett.* **84**, 978 (2004).
- ⁹Y. Nakamura, N. Ikeda, S. Ohkouchi, Y. Sugimoto, H. Nakamura, and K. Asakawa, *Physica E (Amsterdam)* **21**, 551 (2004).
- ¹⁰S. Kohmoto, H. Nakamura, T. Ishikawa, and K. Asakawa, *Appl. Phys. Lett.* **75**, 3488 (1999).
- ¹¹S. Nishikawa, S. Kohmoto, H. Nakamura, T. Ishikawa, K. Asakawa, and O. Wada, *Phys. Status Solidi B* **224**, 521 (2001).
- ¹²S. R. J. Brueck, *Proc. IEEE* **93**, 1704 (2005).
- ¹³A. A. Ukhanov, A. S. Bracker, G. Boishin, and J. C. Culbertson, *J. Vac. Sci. Technol. B* **24**, 1577 (2006).
- ¹⁴S. Birudavolu, S. Q. Luong, N. Nuntawong, Y. C. Xin, C. P. Hains, and D. L. Huffaker, *J. Cryst. Growth* **277**, 97 (2005).
- ¹⁵M. Losurdo, P. Capezzuto, G. Bruno, A. S. Brown, T. Brown, and G. May, *J. Appl. Phys.* **100**, 013531 (2006).
- ¹⁶Y. Tarui, Y. Komiya, and Y. Harada, *J. Electrochem. Soc.* **118**, 118 (1971).
- ¹⁷D. E. Ibbotson, D. L. Flamm, and V. M. Donnelly, *J. Appl. Phys.* **54**, 5974 (1983).
- ¹⁸P. D. Brewer, D. McClure, and R. M. Osgood, *Appl. Phys. Lett.* **47**, 310 (1985).
- ¹⁹W. Qian, M. Skowronski, R. Kaspi, M. D. Graef, and V. P. Dravid, *Appl. Phys. Lett.* **81**, 7268 (1997).
- ²⁰Ch. L. Lin, Y. K. Su, T. S. Se, and W. L. Li, *Jpn. J. Appl. Phys., Part 2* **37**, L1543 (1998).